

Distinct Subdomains of Human Endothelin Receptors Determine Their Selectivity to Endothelin_A-selective Antagonist and Endothelin_B-selective Agonists*

(Received for publication, December 8, 1992)

Aiji Sakamoto, Masashi Yanagisawa†, Tatsuya Sawamura, Taijiro Enoki, Toshio Ohtani, Takeshi Sakurai, Kazuwa Nakao§, Teruhiko Toyooka¶, and Tomoh Masaki||

From the Department of Pharmacology and the §Second Department of Internal Medicine, Faculty of Medicine, Kyoto University, Sakyo-ku, Kyoto 606, Japan, the †Howard Hughes Medical Institute and Department of Molecular Genetics, University of Texas Southwestern Medical Center, Dallas, Texas 75235-9050, and the ¶Second Department of Internal Medicine, Faculty of Medicine, University of Tokyo, Bunkyo-ku, Tokyo 113, Japan

The endothelin (ET) family of peptides acts via two subtypes of G-protein-coupled heptahelical receptors termed ET_A and ET_B, which have distinct rank orders of affinity to endothelin receptor agonists and antagonists. To delineate which portions of the receptor molecules determine ligand selectivity, we have constructed a series of chimeras between human ET_A and ET_B receptors and characterized the chimeric receptors expressed in heterologous cell lines by competitive radioligand binding analysis and by measuring agonist-induced transients of intracellular Ca²⁺. We demonstrate that the binding determinant for the ET_B-selective agonists ET-3, BQ3020, and IRL1620 resides within the region spanning the putative transmembrane helices IV–VI and the adjacent loop regions. In contrast, the transmembrane helices I, II, III, and VII plus the intervening loop regions specify the selectivity for BQ123, an ET_A-selective antagonist. BQ123 exhibited no detectable agonistic activity in all wild-type and chimeric receptors tested. A chimeric receptor that has the transmembrane helices IV–VI (and adjacent loops) from the ET_B receptor inserted into the remaining regions from the ET_A receptor binds both the ET_A- and ET_B-selective ligands with high affinities. Moreover, BQ123 competitively inhibits the binding of the amino-terminally truncated ET_B agonists, [¹²⁵I]-BQ3020 and [¹²⁵I]-IRL1620, to this chimeric receptor, suggesting that BQ123 is a mimic of the carboxyl-terminal linear portion of endothelins. These findings indicate that there are at least two separable ligand interaction subdomains within the endothelin receptors.

(3). They all consist of 21 amino acid residues with two intramolecule disulfide bonds formed between Cys¹-Cys¹⁵ and Cys³-Cys¹¹. The amino acid sequence of each member of the family exhibits a nearly perfect conservation among mammalian species; the only species-related sequence difference known to date is the substitution of Ser⁴ with Asn⁴ in mouse and rat ET-2, which is also called VIC (4). The sequence of the carboxyl-terminal linear portion is shared by all of the members of the mammalian endothelin family; the amino acid substitutions between the isopeptides are clustered in the amino-terminal loop portions, especially within positions 2–7.

Endothelins have a wide variety of biological effects in many different target cell types. Their actions are mediated by specific cell surface receptors that belong to the superfamily of heptahelical G-protein-coupled receptors (5–7). Two subtypes of endothelin receptor, called ET_A and ET_B receptors, have been cloned, and both have been shown in many cell types to activate phospholipase C with resultant intracellular Ca²⁺ transients (8). However, the ET_A and ET_B receptors have distinct cell type/tissue distributions and thus have different physiological roles (9, 10). In many blood vessels, for example, the ET_A receptors reside generally in smooth muscle cells and mediate vasoconstrictor responses, whereas the endothelial cells express the ET_B receptor, which mediates vasodilator effects via the endothelin-induced release of nitric oxide. They can be pharmacologically distinguished by different rank orders of affinity toward endothelin isopeptides; the ET_A receptor is ET-1-selective, showing an affinity rank order of ET-1 ≥ ET-2 >> ET-3, whereas the ET_B receptor exhibits similar affinities to all three isopeptides. In other words, ET-1 can be considered as a nonselective agonist that exhibits similar subnanomolar affinities for both receptor subtypes. ET-3 is a moderately ET_B-selective agonist with the affinity to the ET_B receptor being 2 orders of magnitude higher than that to the ET_A receptor. Recently, a number of synthetic ligands that are highly selective between endothelin receptor subtypes have been developed. For example, the cyclic pentapeptides BQ123, cyclo-(D-Trp-D-Asp-Pro-D-Val-Leu), and BQ153, cyclo-(D-Trp-D-Ala(SO₃)-Pro-D-Val-Leu), act as highly ET_A-selective antagonists (11–13). Among highly ET_B-selective agonists are BQ3020 (*N*-acetyl-[Ala^{11,16}]ET-1(6–21)) (14) and IRL1620 (*N*-succinyl-[Glu⁹,Ala^{11,15}]ET-1(8–21)) (15).

Human ET_A and ET_B receptors exhibit a high polypeptide sequence identity to each other (≈55% overall; ≈74% within the putative transmembrane helices) (16, 17). Since they maintain a clear distinction in ligand binding selectivity de-

The endothelins are a family of potent vasoactive peptides termed endothelin-1, -2 and -3 (ET-1, -2 and -3)¹ (1, 2). The first member of the family, ET-1, was initially described as a potent vasoconstrictor produced by vascular endothelial cells

* This work was supported in part by research grants from the Ministry of Education, Science, and Culture of Japan; the Uehara Memorial Foundation; the Mitsubishi Life Science Foundation; and the Mihara Foundation. The costs of publication of this article were defrayed in part by the payment of page charges. This article must therefore be hereby marked "advertisement" in accordance with 18 U.S.C. Section 1734 solely to indicate this fact.

|| To whom correspondence should be addressed. Tel.: 81-75-753-4477; Fax: 81-75-753-4402.

¹ The abbreviations used are: ET, endothelin; TM, transmembrane helix; ICL, intracellular loop; ECL, extracellular loop.

spite this structural similarity, we set out to localize the subtype-specific determinants within endothelin receptors. We constructed a series of recombinant chimeras between human ET_A and ET_B receptors, expressed them in heterologous cell lines, and characterized those receptors in terms of ligand selectivity by competitive radioligand binding assays and agonist-induced intracellular Ca²⁺ transient assays. We found that the selectivity toward the ET_A-selective antagonist and the ET_B-selective agonist is specified by different subdomains of these receptors.

MATERIALS AND METHODS

Reagents—ET-1 and ET-3 were purchased from Peptide Institute (Osaka, Japan). BQ123 was a generous gift from Banyu Pharmaceutical Co., Ltd. (Tsukuba, Japan). ¹²⁵I-ET-1 and ¹²⁵I-BQ3020 were purchased from Amersham Corp. ¹²⁵I-IRL1620 was a kind gift from Du Pont-New England Nuclear. Fura-2/AM was purchased from Dojin Chemicals (Tokyo, Japan). pME18Sf- vector was a kind gift from Dr. K. Maruyama of the Institute of Medical Science, University of Tokyo.

Chimeric Receptor Constructs—cDNA constructs encoding for chimeric human ET_A/ET_B receptors were assembled by creating common restriction sites within the wild-type receptor cDNAs (16, 17) by oligonucleotide-directed mutagenesis (18) and splicing the desired restriction fragments from the mutated cDNAs. Regions with well conserved amino acid sequences within the putative intracellular loops (ICL I–III) and extracellular loops (ECL I–III) were chosen for creating restriction sites. Care was taken to avoid any amino acid insertions/deletions and to minimize amino acid substitutions at the junction sites as much as possible. The restriction sites introduced and their positions in the deduced amino acid sequences of the ET_A/ET_B receptors, respectively, were as follows (see Fig. 1): *Sna*BI, at Ile⁸²/Ile¹⁰³; *Apa*I, at Pro¹¹⁵/Pro¹³⁶; *Bst*BI, at Asp¹⁴⁹/Gly¹⁷⁰; *Bss*III, at Cys¹⁷⁷/Cys¹⁹³; *Nco*I, at Pro²²⁸/Thr²⁴⁴; *Bgl*II, at Glu²⁸¹/Glu²⁹⁹; *Cla*I, at Arg³⁴⁰/Arg³⁵⁷. The conserved *Eco*RI sites at Asn³⁶¹/Asn³⁷⁸ within the

seventh transmembrane helices (TM VII) of the wild-type receptors were also utilized. Where an amino acid substitution had to be introduced to create a restriction site, we confirmed that the the ligand binding characteristics of the receptors carrying the point mutation alone were indistinguishable from those of the corresponding wild-type receptors (data not shown). The entire coding sequences of the wild-type and chimeric/mutant cDNAs were then subcloned into the SRα promoter-based mammalian expression vector pME18Sf- (19).

Competitive Radioligand Binding Study—COS-7 and *Ltk*⁻ cells were cultured in monolayers in Dulbecco's modified Eagle's medium supplemented with 10% fetal bovine serum. The expression constructs were introduced into COS-7 cells and *Ltk*⁻ cells by the DEAE-dextran method, and the cells were subjected to competitive radioligand binding assays as described (17, 20). 48–72 h after transfection, the monolayers of cells were incubated at 37 for 60 min with 2 × 10⁻¹¹ M ¹²⁵I-Tyr¹³-ET-1, 10⁻¹⁰ M ¹²⁵I-Tyr⁶-BQ3020, or 10⁻¹⁰ M ¹²⁵I-Tyr⁶-IRL1620 (specific activities ≈ 2,000 Ci/mmol) in the presence of various concentrations of cold ET-1, ET-3, or BQ123. After extensive washes, cells were lysed with 0.1 N NaOH, and cell-bound radioactivity was determined. Nonspecific binding was determined in the presence of 10⁻⁶ M unlabeled ET-1 and was approximately 2% of the levels of the specific binding in the absence of the competitor for both cell types.

Measurement of Intracellular Ca²⁺ Transients—We used mouse *Ltk*⁻ cells for Ca²⁺ transient assay in this study because this cell line was found to give highly reproducible, large Ca²⁺ responses to endothelin agonists after transfection with the expression vectors. *Ltk*⁻ cells expressing the wild-type and chimeric receptors 48–72 h after transfection were loaded with the Ca²⁺-sensitive fluorophore Fura-2/AM as described (17). Intracellular Ca²⁺ transients evoked by various concentrations of ET-1 and ET-3 were monitored by a JASCO CAF-110 fluorescence spectrophotometer with dual excitation at 340 nm/380 nm and emission at 500 nm. In some experiments, 10⁻⁶ M BQ123 was added 10 min prior to the addition of the endothelins. The cytosolic concentration of Ca²⁺ ([Ca²⁺]_i) was estimated as described (21). Endothelins induced an acute [Ca²⁺]_i increase in the transfected cells which was followed by lower plateau [Ca²⁺]_i values. The peak [Ca²⁺]_i values from the initial transients were used to draw the dose-response curves.

Data Analysis—All data were the means of at least two independent experiments done in duplicate or triplicate. Raw data obtained from the radioligand binding and Ca²⁺ transient assays were fitted to a logistic equation (22) by using the nonlinear least squares curve-fitting program UltraFit (Biosoft, Inc.). Ligand affinity and the Hill coefficient were designated as parameters for curve fitting. Both in the binding assays and Ca²⁺ transient assays, the estimated Hill coefficients were always close to unity (within the range of 0.86–1.20) for all of the wild-type and chimeric receptors examined, being compatible with one-site ligand/receptor interaction without cooperativity.

RESULTS

Characterization of Wild-type Endothelin Receptors—COS-7 cells transfected with wild-type human ET_A and ET_B receptor cDNA constructs expressed specific binding sites for ¹²⁵I-ET-1 (Fig. 2). The cells transfected with empty vector DNA had no detectable levels of specific ET-1 binding (data not shown). At the ¹²⁵I-ET-1 concentration of 2 × 10⁻¹¹ M, approximately 0.5–1 × 10⁴ molecules/cell of the radioligand were bound in the absence of competitors. The radioligand was displaced in a competitive manner by ET-1, ET-3, or BQ123. ET-1 had a similar binding affinity to both subtypes of receptor: apparent *K_i* values for the ET_A and ET_B receptors were 3.5 × 10⁻⁹ M and 9.5 × 10⁻¹⁰ M, respectively (Table I). ET-3 was virtually equipotent with ET-1 in displacing ¹²⁵I-ET-1 from the ET_B receptor (*K_i* = 2.0 × 10⁻⁹ M), while being nearly 300 times less potent than ET-1 for the ET_A receptor (*K_i* = 1.0 × 10⁻⁶ M). BQ123 was highly selective for ET_A with *K_i* values for the ET_A and ET_B receptors of 2.5 × 10⁻⁶ M and 3.1 × 10⁻⁵ M, respectively. *Ltk*⁻ cells transiently transfected with the same constructs also showed virtually identical ligand binding characteristics. We detected no specific binding of

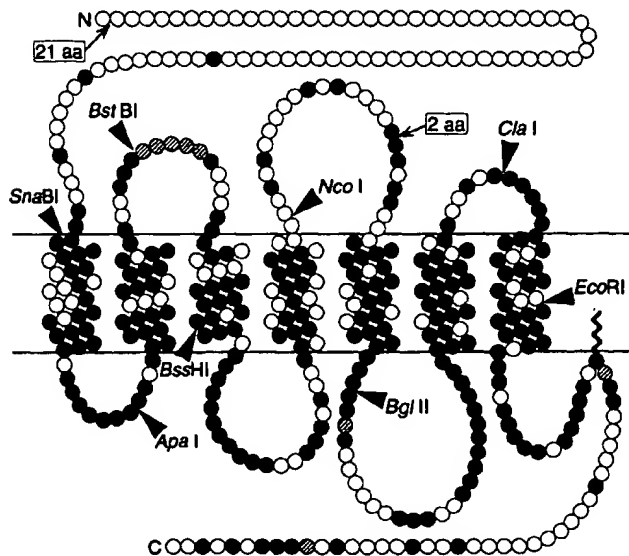


FIG. 1. Predicted transmembrane topography of human endothelin receptors. Amino and carboxyl termini of the cDNA-deduced polypeptides (16, 17) are denoted by N and C, respectively. The number of amino acid residues (circles) is based on the ET_A sequence; the sequence gaps introduced to the ET_B sequence to align the two polypeptides are depicted by striped circles and the insertions by arrows with the number of inserted amino acid (aa) residues in boxes. Closed circles denote the amino acid residues that are identical between the aligned human ET_A and ET_B sequences; open circles designate nonidentical residues. Positions of the restriction sites used to construct chimeric receptors are shown by arrowheads with the names of enzymes. One of the clustered Cys residues within the carboxyl-terminal cytoplasmic tail is assumed to be palmitoylated (wavy line).

FIG. 2. Displacement of [¹²⁵I]-ET-1 binding to COS-7 cells expressing the wild-type ET_A receptor (panel A), the wild-type ET_B receptor (panel B), and chimeric receptor A(N-III)B(IV-VI)A(VII-C) (panel C) by unlabeled ET-1 (●), ET-3 (○), and BQ123 (Δ). Levels of [¹²⁵I]-ET-1 binding are expressed as percentages of the specific binding in the absence of competitor.

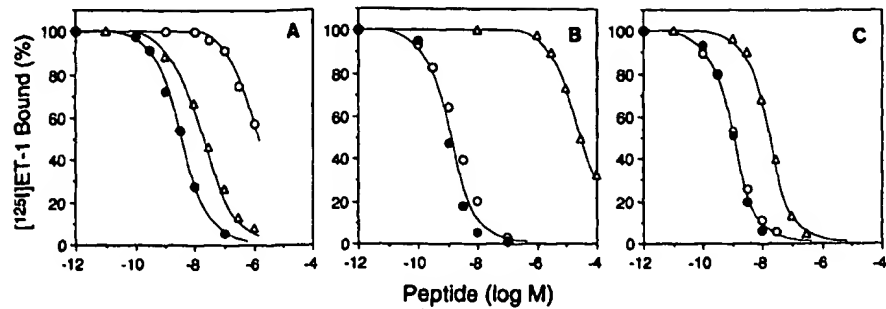


TABLE I

Affinity of ET-1, ET-3, and BQ123 to wild-type and chimeric human endothelin receptors determined by competitive binding assay with [¹²⁵I]-ET-1 as radioligand

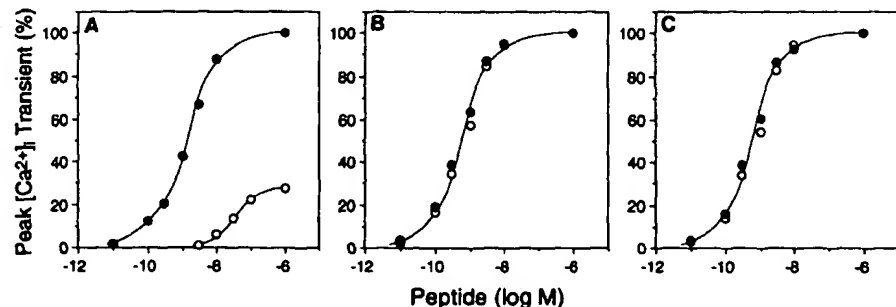
Receptor construct ^a	Affinity K _i			R _{ET-3} ^b	R _{BQ123} ^b
	ET-1	ET-3	BQ123		
		nM			
Wild-type B	0.95	2.0	31,000	2.1	33,000
A(N-I)B(I-C)	0.81	4.1	15,000	5.1	18,000
A(N-I)B(II-C)	0.90	1.5	24,000	1.7	27,000
A(N-II)B(III-C)	0.83	4.8	8,900	5.8	11,000
A(N-III)B(IV-C)	1.7	1.9	200	1.2	120
A(N-IV)B(V-C)	1.0	38	210	38	210
A(N-V)B(VI-C)	1.0	190	130	190	130
A(N-VI)B(VII-C)	2.4	1,100	190	450	79
A(N-VII)B(C)	1.5	930	9.6	610	6.3
Wild-type A	3.5	1,000	25	290	7.1
B(N-I)A(I-C)	1.3	360	25	280	19
B(N-I)A(II-C)	1.4	160	120	120	85
B(N-II)A(III-C)	0.84	120	5,200	140	6,100
B(N-III)A(IV-C)	2.4	1,000	50,000	420	20,000
B(N-IV)A(V-C)	3.3	1,300	51,000	390	16,000
B(N-V)A(VI-C)	0.93	51	35,000	55	37,000
B(N-VI)A(VII-C)	1.0	6.2	41,000	6.0	40,000
B(N-VII)A(C)	1.2	4.1	19,000	3.4	16,000
A(N-III)B(IV-VI)A(VII-C)	1.0	1.1	20	1.1	20
B(N-IV)A(V)B(VI-C)	0.88	38	16,000	43	19,000
B(N-I)A(II-III)B(IV-C)	3.0	ND ^c	1,400	ND	480
B(N-I)A(II-III)B(IV-VI)A(VII)B(C)	1.1	ND	300	ND	270
B(N-I)A(II-III)B(IV-VI)A(VII)B(C)	3.4	ND	41	ND	12

^a N, I-VII, and C designate the amino-terminal extracellular tail, transmembrane helices I-VII, and carboxyl-terminal cytoplasmic tail, respectively, plus the adjacent loop regions when applicable (see Fig. 1). A(...) and B(...) denote that the chimeric receptor has ET_A and ET_B sequences within the designated portions, respectively.

^b R_{ET-3} = K_i(ET-3)/K_i(ET-1); R_{BQ123} = K_i(BQ123)/K_i(ET-1).

^c ND, not determined.

FIG. 3. Dose-response relationships of [Ca²⁺]_i transients evoked by ET-1 (●) and ET-3 (○) in Ltk⁻ cells expressing the wild-type ET_A receptor (panel A), the wild-type ET_B receptor (panel B), and chimeric receptor A(N-III)B(IV-VI)A(VII-C) (panel C). Initial peak [Ca²⁺]_i increments are plotted as percentages of the maximum [Ca²⁺]_i increments produced by ET-1 (10⁻⁸ M) in cells expressing the wild-type ET_A receptor.



[¹²⁵I]-ET-1 in Ltk⁻ cells transfected with the empty vector DNA (data not shown).

ET-1 and ET-3 produced [Ca²⁺]_i transient responses in Ltk⁻ cells transfected with the endothelin receptor constructs but not in the cells transfected with the empty vector plasmid. Fig. 3 shows the dose-response relationships for the initial

peak increments of [Ca²⁺]_i evoked by ET-1 and ET-3 in the transfected Ltk⁻ cells. ET-1 exhibited approximately equal potency toward both receptor subtypes; the agonist concentrations that elicited half-maximum response (EC₅₀) for the ET_A and ET_B receptors were 1.3 × 10⁻⁹ M and 4.9 × 10⁻¹⁰ M, respectively. Although ET-3 was almost equipotent with ET-

1 toward the ET_B receptor ($EC_{50} = 6.0 \times 10^{-10}$ M), it was 25 times less potent than ET-1 for ET_A ($EC_{50} = 3.3 \times 10^{-8}$ M). Furthermore, ET-3 produced a considerably smaller maximum response for ET_A-expressing cells as compared with ET-1; the maximum responses to ET-3 (at 10^{-6} M) were 28 and 100% of those to ET-1 in the cells expressing the ET_A and ET_B receptors, respectively. In the ET_A-expressing cells, BQ123 (10^{-6} M) inhibited an ET-1 (10^{-6} M)-induced $[Ca^{2+}]_i$ increase by 95% (Fig. 4). In contrast, the same concentration of the antagonist inhibited an ET-1 (10^{-6} M)-induced Ca^{2+} response by only 9% in the cells expressing the ET_B receptor. BQ123 at up to 10^{-4} M had no detectable agonist activity for either receptor subtype in this assay (data not shown).

Characterization of Chimeric Receptors—We constructed two systematic series of chimeric endothelin receptors by progressively substituting the structure of the ET_A receptor with that of the ET_B receptor (see "Materials and Methods"). The progressive substitutions from the carboxyl terminus resulted in the series of A/B chimeras, whereas the amino-terminal substitutions gave rise to B/A chimeras. Thus, for example, chimera A(N-II)B(III-C) hereafter designates a chimeric receptor consisting of the ET_A sequence from the amino-terminal putative extracellular tail through the TM II, followed by the ET_B sequence from the TM III through the carboxyl-terminal cytoplasmic tail. Each chimeric molecule was expressed in COS-7 cells, and the cells were subjected to a competitive radioligand binding assay. All chimeric receptor constructs we tested conferred similar densities of ^{125}I -ET-1 binding sites in these cells; between 0.5 and 1×10^4 molecules/cell of ^{125}I -ET-1 (at 2×10^{-11} M) were bound in the absence of competitors. Table I summarizes the apparent K_i values of the competitors determined for the wild-type and chimeric receptors expressed in COS-7 cells. The K_i values for ET-1 were similar in the wild-type and all chimeric receptors, all being within the range from 8.1×10^{-10} M to 3.5×10^{-9} M. Provided with this uniformity of the affinity to ET-1 in all chimeric receptors, we divided the K_i values for ET-3 and BQ123 by those for ET-1 in each receptor construct and used these affinity ratios (designated hereafter as R_{ET-3} and R_{BQ123} , respectively) as an indicator of the ligand selectivity exhibited by each recombinant receptor (Table I).

Determinant for Selectivity to BQ123—Replacement of the amino-terminal extracellular tail of ET_A with the corresponding region of ET_B caused little change in the affinity to BQ123 (chimera B(N)A(I-C)). However, further progressive replace-

ment of the TM I, II, and III of ET_A (including the intervening loops) with the corresponding regions from ET_B resulted in a progressive increase in K_i values for BQ123 and thus in R_{BQ123} values (chimeras B(N-I)A(II-C), B(N-II)A(III-C), and B(N-III)A(IV-C)). Replacement of the carboxyl-terminal half of TM VII together with the carboxyl-terminal cytoplasmic tail of ET_A with the corresponding region of ET_B caused no significant change in BQ123 selectivity (chimera A(N-VII)B(C)). Further substitution of the amino-terminal half of TM VII plus the carboxyl-terminal half of ECL III resulted in an 11-fold increase in the R_{BQ123} value (chimera A(N-VI)B(VII-C)). The selectivity to BQ123 did not change very much when further substitution of the ET_A sequence from the carboxyl-terminal side was carried out through TM IV and ICL II (chimeras A(N-V)B(VI-C), A(N-IV)B(V-C), and A(N-III)B(IV-C)). However, when the TM III together with the carboxyl-terminal half of ECL I was further substituted (chimera A(N-II)B(III-C)), an additional ≈ 100 -fold increase of R_{BQ123} was observed.

These results suggest that the ET_A sequences spanning from TM I through TM III as well as the amino-terminal half of TM VII are likely to be important for its high affinity binding to BQ123. To test whether these regions were also sufficient to define the binding determinant for the ET_A-selective antagonist, we constructed the chimeras B(N)A(I-III)B(IV-VI)A(VII)B(C). This chimeric receptor indeed exhibited the ability to bind BQ123 with high affinity, with an R_{BQ123} value similar to that for the wild-type ET_A receptor (Table I and Fig. 5). Furthermore, BQ123 (10^{-6} M) inhibited the ET-1-induced Ca^{2+} transient response by 96% in *Ltk*⁻ cells transfected with this chimeric construct (Fig. 4). BQ123 showed no detectable agonist activity at up to 10^{-4} M. Although the chimera B(N)A(I-III)B(IV-VI)A(VII)B(C) maintained high affinity to BQ123, two additional chimeras (B(N-I)A(II-III)B(IV-C) and B(N-I)A(II-III)B(IV-VI)A(VII)B(C)) exhibited intermediate binding affinities to BQ123, indicating that the structures of TM I and TM VII from the ET_A receptor indeed contributed to the high affinity binding of BQ123.

Determinant for Selectivity to ET-3—Progressive replacement of the sequence of the ET_B receptor with that of ET_A from the amino-terminal extracellular tail through TM III caused little changes in R_{ET-3} values (chimeras A(N)B(I-C), A(N-I)B(II-C), A(N-II)B(III-C), and A(N-III)B(IV-C)). However, when the ICL II and TM IV were further substituted with the corresponding parts of ET_A, the R_{ET-3} value increased to 38 (chimera A(N-IV)B(V-C)). Further substitution with the ET_A sequence made the resultant chimeras indistinguishable

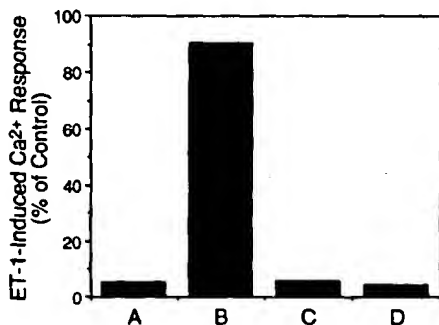


FIG. 4. Inhibition of ET-1-induced $[Ca^{2+}]_i$ transients by BQ123 (10^{-6} M) in *Ltk*⁻ cells expressing the wild-type ET_A receptor (A), the wild-type ET_B receptor (B), chimeric receptor A(N-III)B(IV-VI)A(VII-C) (C), and chimeric receptor B(N)A(I-III)B(IV-VI)A(VII)B(C) (D). BQ123 was applied 10 min prior to the challenge with 10^{-6} M ET-1. Initial peak $[Ca^{2+}]_i$ increments in the presence of BQ123 are expressed as percentages of the $[Ca^{2+}]_i$ increments seen in the absence of the antagonist.

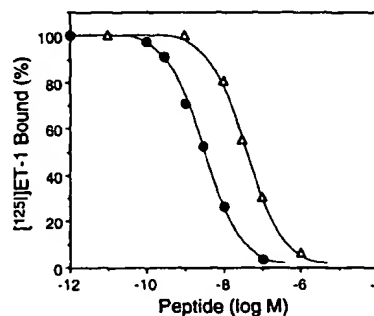


FIG. 5. Displacement of ^{125}I -ET-1 binding to COS-7 cells expressing chimeric receptor B(N)A(I-III)B(IV-VI)A(VII)B(C) by unlabeled ET-1 (●) and BQ123 (Δ). Levels of ^{125}I -ET-1 binding are plotted as percentages of the specific ^{125}I -ET-1 binding in the absence of competitor.

from the wild-type ET_A receptor in terms of R_{ET-3} values. Similarly, progressive replacement of the ET_B sequence with ET_A from the carboxyl-terminal cytoplasmic tail through the carboxyl-terminal half of ECL III (chimeras B(N-VII)A(C) and B(N-VI)A(VII-C)) resulted in little change in R_{ET-3} . However, further substitution of the amino-terminal half of ECL III, TM VI, and most of ICL III with the ET_A sequence caused a significant increase of the selectivity ratio to 55 (chimera B(N-V)A(VI-C)).

These results suggest that the structure of the ET_B receptor spanning ICL II through the amino-terminal half of ECL III was necessary to render the receptor able to bind ET-3 with high affinity. To confirm further that the above mentioned region from the ET_B receptor is sufficient to provide high affinity binding of ET-3, we constructed the chimera A(N-III)B(IV-VI)A(VII-C). Indeed, this chimeric receptor had virtually equal affinities for ET-1 and ET-3 both in the radioligand binding assay and in the $[Ca^{2+}]_i$ transient assay (Table I and Figs. 2 and 3). In contrast, the chimeric receptor B(N-IV)A(V)B(VI-C) displayed an intermediate affinity to ET-3; its R_{ET-3} value was 7 times lower than the wild-type ET_A yet 20 times higher than the ET_B. This indicates that although the sequence of the ET_B receptor spanning ECL II and TM V significantly contributes to the binding determinant for ET-3, this structure alone is not sufficient to form the complete determinant.

There are two charge-modifying amino acid substitutions between the ET_A and ET_B receptors in their TM IV and TM VI: namely, Asp²⁴¹ and Leu³⁴⁷ in ET_B versus Val²²⁶ and Lys³³⁰ in ET_A. To examine if these substitutions of charged residues have any effect on the binding affinity of ET-3, we introduced the following point missense mutations at these positions: ET_B(D241V), ET_B(L347K), ET_B(D241V/L347K), ET_A(V225D), ET_A(K330I), ET_A(V225D/K330I). However, we found that the ET-3 selectivities of these mutant receptors were all indistinguishable from the respective wild-type receptors (data not shown).

A Chimeric Receptor with High Affinity to Both ET_A and ET_B-selective Ligands—Since TM I, II, III and VII from the ET_A receptor (including the intervening loop regions) were sufficient to form the high affinity binding determinant for BQ123 in the chimeric receptors, we expected that the "ET_B-like" chimera A(N-III)B(IV-VI)A(VII-C) could still maintain high affinity to BQ123. This was actually the case; the chimeric receptor had an affinity to BQ123 which was very similar to native ET_A receptor (Table I and Fig. 2). Therefore, it seemed that this particular chimeric receptor could accept both ET_A- and ET_B-selective ligands with high affinity. We performed competitive binding studies on this chimeric construct by using the highly ET_B-selective agonists ¹²⁵I-BQ3020 and ¹²⁵I-IRL1620 as radioligands and the highly ET_A-selective antagonist BQ123 as competitor. We found that the chimeric receptor specifically bound these ET_B-selective radioligands in a manner similar to the native ET_B receptor (Fig. 6). Moreover, the specific binding of the ET_B-selective radioligands was completely abolished by 10⁻⁶ M BQ123 in the chimeric receptor (Fig. 6). In contrast, in the case of the wild-type ET_B receptor, the radioligand binding was affected by 10⁻⁶ M BQ123 only slightly. The apparent K_i values for BQ123 in displacing the specific binding of ¹²⁵I-BQ3020 and ¹²⁵I-IRL1620 in the chimeric receptor were 1.9×10^{-8} M and 1.0×10^{-8} M, respectively (Fig. 7). These values were similar to the K_i values for BQ123 observed in the wild-type ET_A receptor by using ¹²⁵I-ET-1 as radioligand (Table I and Fig. 2).

We further examined whether BQ123 still acted as an antagonist for the chimeric receptor A(N-III)B(IV-VI)A(VII-

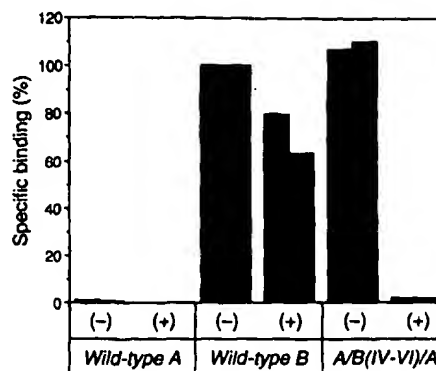


FIG. 6. Specific binding of the ET_B-selective ligand ¹²⁵I-BQ3020 (filled bars) and ¹²⁵I-IRL1620 (striped bars) to COS-7 cells expressing the designated receptor constructs. Cells were separately incubated with each labeled peptide (10⁻¹⁰ M) in the absence (-) and presence (+) of 10⁻⁶ M BQ123. Levels of specific binding are expressed as percentages of those seen in the wild-type ET_B receptor in the absence of BQ123.

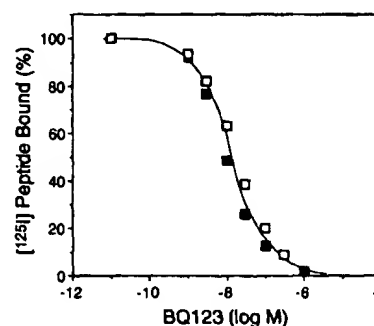


FIG. 7. Displacement by BQ123 of ¹²⁵I-BQ3020 (□) and ¹²⁵I-IRL1620 (■) binding to COS-7 cells expressing chimeric receptor A(N-III)B(IV-VI)A(VII-C). Levels of specific binding of the radioligands are plotted as percentages of the specific binding in the absence of BQ123.

C). BQ123 (10⁻⁶ M) inhibited the Ca²⁺ transients induced by 10⁻⁹ M ET-1 by 95% in Ltk⁻ cells expressing the chimeric receptor (Fig. 4). BQ123 did not have a detectable agonist activity at up to 10⁻⁴ M.

DISCUSSION

All of the chimeric receptor constructs we examined in this study conferred similar densities of specific ¹²⁵I-ET-1 binding sites when expressed in COS-7 cells. Furthermore, all chimeric receptors exhibited high affinities to ET-1 which were comparable with those observed in the wild-type ET_A and ET_B receptors. Taken together with the fact that ET-1 is a non-selective ligand for both receptor subtypes, these findings suggest that the details of tertiary structure of the ET_A and ET_B receptors are similar to each other and well maintained in all chimeric receptors tested. This may at least partly be because of the high level of polypeptide sequence similarity seen between the two receptor subtypes. By systematically constructing and analyzing chimeric endothelin receptors exhibiting these prerequisite properties, we demonstrated the clearly distinct binding determinants for subtype-selective agonists and antagonists. A separation of agonist and antagonist binding sites has recently been reported for human progesterone receptor (23). It is of interest to examine whether the complete separation of agonist and antagonist binding determinants can be seen also in other family of heptahelical G-protein-coupled receptors, especially in receptors for other

peptide ligand families such as tachykinins (24).

The amino acid sequences of the ET_A and ET_B receptors are most dissimilar to each other in their putative amino-terminal extracellular tails, which have predicted *N*-glycosylation sites. In fact, there is no detectable sequence similarity between these portions of the two receptor subtypes at all. It is therefore somewhat surprising that mutual swapping of the extracellular tails between the ET_A and ET_B receptors had no appreciable effect on their ligand binding characteristics (chimeras B(N)A(I-C) and A(N)B(I-C)). The function of these parts of the receptor molecules is not clear at present; one possibility is that they may assist the receptor polypeptides to fold and be expressed on the cell surface in the proper transmembrane orientations.

BQ123 is an established competitive antagonist selective for the ET_A receptor (11). The three-dimensional structures of BQ123 and ET-1 in solution have been demonstrated with proton NMR by several independent laboratories (25–28). However, so far it has been unclear as to which part of the ET-1 structure may be mimicked by the antagonist. We demonstrated in this study that the chimeric receptor A(N-III)B(IV-VI)A(VII-C) could achieve a high affinity binding of both BQ123 and the two ET_B-selective agonists, BQ3020 and IRL-1620. Furthermore, we found that BQ123 could compete with iodinated BQ3020 or IRL1620 for the specific binding to this chimeric receptor. The latter ligands are linear, amino-terminally truncated derivatives of ET-1. These findings strongly argue for the idea that BQ123 mimicks a structure within the carboxyl-terminal, linear portion of ET-1. In this regard, the amino acid sequence of BQ123 appears to have certain similarity to the carboxyl-terminal sequence of ET-1. The motif found in BQ123, -D-Val-Leu-D-Trp-D-Asp, may mimic the carboxyl terminus of endothelins, -Ile-Ile-Trp-COOH. We also demonstrated that the determinant for the high affinity binding of BQ123 resides within the TM I-III and VII (including adjacent loops) of the ET_A receptor. This is in agreement with the findings recently reported by Adachi *et al.* (29) that the ECL I from the ET_A receptor is an important determinant for BQ123 binding. Taken together with the above argument, it seems plausible to consider that these portions of the receptor molecules contain at least a part of their binding domain for the carboxyl termini of endothelins, which includes the Trp²¹ residue essential for the binding of the peptide to either receptor subtype (30).

We have demonstrated that the TM IV-VI and the adjacent loop regions of the ET_B receptor constitute the high affinity binding determinant for the ET_B-selective agonists, including the amino-terminally truncated linear ET-1 derivatives. This is in sharp contrast to the case of the heptahelical receptors for tachykinins, in which the region spanning from TM II to ECL II (together with a minor contribution of the amino-terminal tail) has been recently reported to specify isopeptide selectivity (24). It is interesting to note that, like endothelin family, tachykinins have a common carboxyl-terminal motif and divergent amino-terminal portions. These observations indicate a significant difference in the mode of receptor/ligand interactions between the endothelin and tachykinin systems, despite these apparent similarities in the general configurations of isopeptides and receptors.

The findings presented in this study provide further insight into the possible mechanism for the ligand selectivity of endothelin receptors. It is plausible to consider that the structures of endothelin isopeptides and their derivatives are comprised of two distinct subdomains: the amino-terminal disulfide loop portion that is variable among isopeptides, and the carboxyl-terminal linear hydrophobic region that is highly

conserved. The currently available information on the structure-activity relations of endothelin derivatives suggests the following general rules (30, 31): (i) *both* the amino-terminal loop structure from ET-1 (or other nonselective ligands such as sarafotoxin S6b) *and* the common carboxyl-terminal linear structure are required for high affinity binding to the ET_A receptor; (ii) in contrast, the ET_B receptor only requires the carboxyl-terminal half of the ligand. In this context, the present results suggest that the TM IV-VI of endothelin receptors may interact with the amino-terminal loop portion of the ligands. Incorporating these considerations, we present a hypothetical model for the binding determinants of endothelin receptors and their ligands (Fig. 8). Thus, it is conceivable that the amino-terminal loop domain of ET-1 functions in a manner similar to a classical "address" domain suggested for a number of peptide ligand family (32). The TM IV-VI of the ET_A receptor interacts selectively with this address domain of ET-1 to promote a full activation of receptor, which is brought about by the carboxyl-terminal "message" domain of ET-1. However, the corresponding address domains of the ET_B-selective ligands are either invalid (ET-3) or missing (BQ3020, IRL1620), resulting in the inability to interact with the ET_A receptor. In contrast, the ET_B receptor, with its subtly different structures within the TM IV-VI region, may be highly promiscuous for the ligands' address domains. Alternatively, it is tempting to speculate that the TM IV-VI domain of the ET_B receptor may function as a self-contained address recognition domain that does not require a valid address information presented by the ligand. Further, it is also conceivable that the mode of interaction between the cyclic pentapeptide antagonist BQ123 and the ET_A receptor

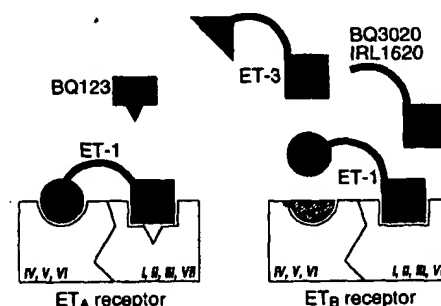


FIG. 8. A hypothetical model for the interaction of endothelin receptor subtypes with their ligands. Endothelin agonists are presumably comprised of the carboxyl-terminal message sequence common to all of the natural and synthetic isopeptides (filled squares) coupled with the amino-terminal address domain, which involves the disulfide loop portion of the isopeptides. The region spanning the TM IV-VI (and the intervening loop portions) of the ET_A receptor interacts with the address domain specific to ET-1. ET-3 has an address domain that can interact only weakly with this address recognition subdomain of the ET_A receptor. The highly ET_B-selective agonists BQ3020 and IRL1620 have no valid address domain because of the amino-terminal truncations. However, in the case of the ET_B receptor, the corresponding address recognition subdomain can interact with a much wider spectrum of ligands' address portions. Alternatively, the ET_B receptor presumably has an internal, self-content address domain (depicted with a striped hemisphere) so that it requires no external address sequence. The cyclic pentapeptide antagonist BQ123 interacts with the subdomain of the ET_A receptor covering the TMs I-III and VII plus the adjacent loop portions (note that despite the apparent separation of these transmembrane helices in the primary structure, they are presumably contiguous to each other in the tertiary structure common to the rhodopsin superfamily (5)). However, because of a subtle difference in the mode of binding, the antagonist is unable to evoke the conformational alteration necessary to activate the receptor and also becomes exempt from the requirement of interactions at the address domain.

is significantly different from agonist/receptor interactions so that it does not require the interaction at the addressing domain.

Acknowledgments—We thank Drs. Mitsuo Yano and Masaki Ihara of Banyu Pharmaceutical Co. Ltd. for samples of BQ123. We also thank Dr. Kazuo Maruyama of the Institute of Medical Science, University of Tokyo, and Dr. Beverly Brown of Du Pont-New England Nuclear for the expression vector pME18Sf- and iodinated IRL1620, respectively.

REFERENCES

- Inoue, A., Yanagisawa, M., Kimura, S., Kasuya, Y., Miyauchi, T., Goto, K., and Masaki, T. (1989) *Proc. Natl. Acad. Sci. U. S. A.* **86**, 2863-2867
- Masaki, T., Yanagisawa, M., and Goto, K. (1992) *Med. Res. Rev.* **12**, 391-421
- Yanagisawa, M., Kurihara, H., Kimura, S., Tomobe, Y., Kobayashi, M., Mitsui, Y., Yazaki, Y., Goto, K., and Masaki, T. (1988) *Nature* **332**, 411-415
- Saida, K., and Mitsui, Y. (1991) *J. Cardiovasc. Pharmacol.* **17**, (Suppl. 7) 55-58
- Jackson, T. (1991) *Pharmacol. Ther.* **50**, 425-442
- Dohlman, H. G., Thorner, J., Caron, M. G., and Lefkowitz, R. J. (1991) *Annu. Rev. Biochem.* **60**, 653-688
- Strosberg, A. D. (1991) *Eur. J. Biochem.* **196**, 1-10
- Sakurai, T., Yanagisawa, M., and Masaki, T. (1992) *Trends Pharmacol. Sci.* **13**, 103-108
- Hori, S., Komatsu, Y., Shigemoto, R., Mizuno, N., and Nakanishi, S. (1992) *Endocrinology* **130**, 1885-1895
- Nakamichi, K., Ihara, M., Kobayashi, M., Saeki, T., Ishikawa, K., and Yano, M. (1992) *Biochem. Biophys. Res. Commun.* **182**, 144-150
- Ihara, M., Noguchi, K., Saeki, T., Fukuroda, T., Tsuchida, S., Kimura, S., Fukami, T., Ishikawa, K., Nishikibe, M., and Yano, M. (1992) *Life Sci.* **50**, 247-255
- Ishikawa, K., Fukami, T., Nagase, T., Fujita, K., Hayama, T., Niiyama, K., Mase, T., Ihara, M., and Yano, M. (1992) *J. Med. Chem.* **35**, 2139-2142
- Fukuroda, T., Nishikibe, M., Ohta, Y., Ihara, M., Yano, M., Ishikawa, K., Fukami, T., and Ikemoto, F. (1992) *Life Sci.* **50**, PL107-PL112
- Ihara, M., Saeki, T., Fukuroda, T., Kimura, S., Ozaki, S., Patel, A. C., and Yano, M. (1992) *Life Sci.* **51**, PL47-PL52
- Watakabe, T., Urade, Y., Takai, M., Uemura, I., and Okada, T. (1992) *Biochem. Biophys. Res. Commun.* **185**, 867-873
- Hosoda, K., Nakao, K., Arai, H., Suga, S., Ogawa, Y., Mukoyama, M., Shirakami, G., Saito, Y., Nakanishi, S., and Imura, H. (1991) *FEBS Lett.* **287**, 23-26
- Sakamoto, A., Yanagisawa, M., Sakurai, T., Takuwa, Y., Yanagisawa, H., and Masaki, T. (1991) *Biochem. Biophys. Res. Commun.* **178**, 656-663
- Kunkel, T. A. (1986) *Proc. Natl. Acad. Sci. U. S. A.* **82**, 488-492
- Takebe, Y., Seiki, M., Fujisawa, J., Hoy, P., Yokota, K., Arai, K., Yoshida, M., and Arai, N. (1988) *Mol. Cell. Biol.* **8**, 466-472
- Sakurai, T., Yanagisawa, M., Takuwa, Y., Miyazaki, H., Kimura, S., Goto, K., and Masaki, T. (1990) *Nature* **348**, 732-735
- Gryniewicz, G., Ponie, M., and Tsien, R. Y. (1985) *J. Biol. Chem.* **260**, 3440-3450
- DeLean, A., Munson, P. J., and Rodbard, D. (1978) *Am. J. Physiol.* **235**, 97-102
- Vegeto, E., Allan, G. F., Schrader, W. T., Tsai, M.-J., McDonnell, D. P., and O'Malley, B. W. (1992) *Cell* **69**, 703-713
- Yokota, Y., Akazawa, C., Ohkubo, H., and Nakanishi, S. (1992) *EMBO J.* **11**, 3585-3591
- Atkinson, R. A., and Pelton, J. T. (1992) *FEBS Lett.* **296**, 1-6
- Krystek, S. R., Jr., Bassolino, D. A., Brucoleri, R. E., Hunt, J. T., Porubcan, M. A., Wandler, C. F., and Andersen, N. H. (1992) *FEBS Lett.* **299**, 255-261
- Reily, M. D., Thanabal, V., Omecinsky, D. O., Dunbar, J. B., Jr., Doherty, A. M., and DePue, P. L. (1992) *FEBS Lett.* **300**, 136-140
- Andersen, N. H., Chen, C. P., Marschner, T. M., Krystek, S. R., Jr., and Bassolino, D. A. (1992) *Biochemistry* **31**, 1280-1295
- Adachi, M., Yang, Y.-Y., Trzeciak, A., Furuichi, Y., and Miyamoto, C. (1992) *FEBS Lett.* **311**, 179-183
- Doherty, A. M. (1992) *J. Med. Chem.* **35**, 1495-1508
- Urade, Y., Fujitani, Y., Oda, K., Watakabe, T., Umemura, I., Takai, M., Okada, T., Sakata, K., and Karaki, H. (1992) *FEBS Lett.* **311**, 12-16
- Takemori, A. E., and Portguese, P. S. (1992) *Annu. Rev. Pharmacol. Toxicol.* **32**, 239-269